Stretchable Wire-Shaped Asymmetric Supercapacitors Based on Pristine and MnO_2 Coated Carbon Nanotube Fibers

Ping Xu,[†,‡] Bingqing Wei,[‡] Zeyuan Cao,[‡] Jie Zheng,[§] Ke Gong,[§] Faxue Li,[†] Jianyong Yu,[*,†] Qingwen Li,[∥] Weibang Lu,[∥] Joon-Hyung Byun,[⊥] Byung-Sun Kim,[⊥] Yushan Yan,[§] and Tsu-Wei Chou[*,‡]

[†]College of Textiles, Donghua University, Shanghai, 201620, P. R. China, [‡]Department of Mechanical Engineering, University of Delaware, Newark, Delaware 19716, United States, [§]Department of Chemical and Biomolecular Engineering, Center for Catalytic Science and Technology, University of Delaware, Newark, Delaware 19716, United States, [∥]Suzhou Institute of Nano-Tech and Nano-Bionics, Suzhou 215123, P. R. China, and [⊥]Composites Research Center, Korean Institute of Materials Science, Changwon, 641831, South Korea

ABSTRACT While the emerging wire-shaped supercapacitors (WSS) have been demonstrated as promising energy storage devices to be implemented in smart textiles, challenges in achieving the combination of both high mechanical stretchability and excellent electrochemical performance still exist. Here, an asymmetric configuration is applied to the WSS, extending the potential window from 0.8 to 1.5 V, achieving tripled energy density and doubled power density compared to its asymmetric counterpart while accomplishing stretchability of up to 100% through the prestrainning-then-buckling approach. The stretchable asymmetric WSS constituted of MnO_2/CNT hybrid fiber positive electrode, aerogel CNT fiber negative electrode and KOH-PVA electrolyte possesses a high specific capacitance of around 157.53 μF cm^{-1} at 50 mV s^{-1} and a high energy density varying from 17.26 to 46.59 nWh cm^{-1} with the corresponding power density changing from 7.63 to 61.55 μW cm^{-1}. Remarkably, a cyclic tensile strain of up to 100% exerts negligible effects on the electrochemical performance of the stretchable asymmetric WSS. Moreover, after 10 000 galvanostatic charge–discharge cycles, the specific capacitance retains over 99%, demonstrating a long cyclic stability.

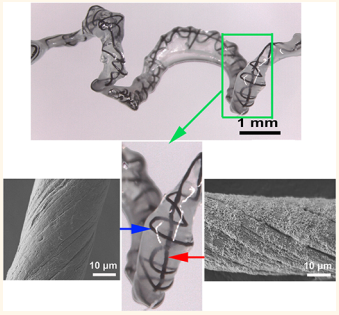

KEYWORDS: asymmetric configuration · stretchability · wire-shaped supercapacitors · carbon nanotube fibers · manganese oxides

In addition to their primary functions, wearable electronics and smart clothes can not only store the energy harvested from sunlight, body heat ,and body movements but also deliver power to electronic devices.[1] Strategies for developing energy storage textiles have been widely reported:[2−4] textiles are directly used as two-dimensional substrates to carry electrochemical active materials;[5−9] or energy storage systems are fabricated in one-dimensional wire shape by twisting together two conductive fibers or assembling active materials in a core–shell structure.[10−33] The wire-shaped energy storage devices have distinct advantages over the planar counterparts in the development of lightweight, reconfigurable, and portable electronics.[27] Most importantly, a wire-shaped device can be integrated with the well-developed textile technology in a highly versatile manner.[23,27]

Currently, stretchability has been achieved in various electronics, ranging from conductors, sensors, solar cells and batteries to organic light-emitting diodes.[34,35] Aiming at applications in wearable electronics, the realization of stretchability has become a research topic of high priority for wire-shaped supercapacitors (WSSs). So far, there are only a few papers addressing stretchable WSSs. Meng *et al.* fabricated a spring-like supercapacitor consisting of two all-graphene core–sheath fibers twisted together and demonstrated excellent properties of the resulting stretchable supercapacitors.[29] Taking advantage of the large elastic deformation of Spandex fiber as well as the intrinsic properties of carbon nanotube fibers (high conductivity, excellent flexibility and chemical inertness),[36−38] we studied a stretchable carbon nanotube (CNT) fiber based WSS which can sustain outstanding electrochemical performance even at cyclic tensile strains of up to 100%.[32] Yang *et al.* demonstrated a stretchable WSS by sequently wrapping two layers of gel-electrolyte-separated aligned carbon nanotube sheet on an elastic fiber.[33] Recently, a freestanding stretchable supercapacitor was

* Address correspondence to yujy@dhu.edu.cn, chou@udel.edu.

Received for review February 25, 2015 and accepted May 11, 2015.

Published online May 11, 2015
10.1021/acsnano.5b01244

fabricated by two parallel spring-like CNT fibers and it can withstand tensile strain reaching 100%.[39] An extremely stretchable WSS with a stretchability of up to 350% and a capacitance of 8.0 F g^{-1} at 0.5 A g^{-1} was also reported.[40]

However, apart from the achievements of stretchable WSS mentioned above, such supercapacitors still suffer from the low capacitance, low working potential (usually 0.8 V), and thus low energy and power densities, preventing them from practical applications. Therefore, it is imperative to develop an effective approach to enhance the electrochemical performance, while maintaining their high stretchability of WSSs.

The asymmetric electrode configuration, taking advantage of the pseudocapacitive positive electrode to improve the specific capacitance as well as the nanocarbon negative electrode to extend the operating voltage, has been demonstrated as an effective means for improving the supercapacitor electrochemical performance.[41−44] The higher operating voltage can not only enhance the energy density ($E = CV^2/2$; E, energy density; C, capacitance; and V, operating voltage), but also reduce the number of capacitors in series to achieve expected output voltage.[45]

Lately, asymmetric electrode configuration has been applied to the newly emerged WSSs. A fiber-based flexible all-solid state asymmetric supercapacitor using titanium wire/Co_3O_4 nanowires and carbon fibers/graphene electrodes was demonstrated to enhance both stored energy and delivered power by at least 1860%.[41] Dong *et al.* used $Ni(OH)_2$-nanowire and ordered mesoporous carbon electrodes to prepare wire-shaped flexible asymmetric supercapacitor, which displayed high capacitance of 35.67 mF cm^{-2} and energy density of 0.01 mWh cm^{-2}.[46] An asymmetric supercapacitor based on CNT yarn and MnO_2/CNT hybrid fiber was also reported to have a superior electrochemical performance to its symmetric counterparts.[47] However, to the best of our knowledge, an asymmetric WSS, which shows simultaneously excellent electrochemical performance and high stretchability, has not been reported.

Herein, an asymmetric supercapacitor with MnO_2/CNT hybrid fiber as the positive electrode and pristine aerogel CNT fiber as the negative electrode, and KOH-poly(vinyl alcohol) (KOH-PVA) gel electrolyte has been fabricated. The elaborative selection of MnO_2 is due to its abundance, low cost, low toxicity, friendly interfacial properties with carbon materials, and a high theoretical pseudocapacitance (about 1370 F g^{-1}).[48,49] The asymmetric WSS with stretchability of up to 100% possesses a high potential window of 1.5 V, a high specific capacitance (157.53 μF cm^{-1}), a high energy density (17.26−46.59 nWh cm^{-1}), and a high cycling stability.

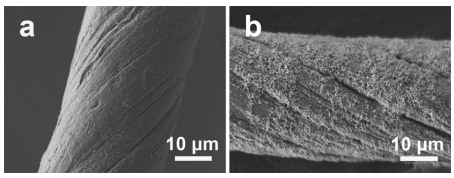

Figure 1. SEM morphologies of (a) pristine CNT fiber electrode and (b) MnO_2/CNT hybrid fiber electrode.

RESULTS AND DISCUSSION

The aerogel CNT fiber composed of numerous carbon nanotubes twisted together has a compact structure with a diameter of about 31.0 μm, as shown in Figure 1a. The MnO_2/CNT hybrid fiber positive electrode shown in Figure 1b was prepared by precipitating nanostructured MnO_2 particles on the aerogel CNT fiber from the potassium permanganate ($KMnO_4$) precursor. The procedures are depicted in the Experimental Section. The MnO_2 particles precipitated using this method was demonstrated to possess nanoscale architectures.[50−53]

Figure 2a shows the element distribution on the MnO_2/CNT hybrid fiber. Carbon, manganese, and oxygen were uniformly distributed on the fiber surface. Potassium and iron were also detected in the EDX spectrum of Figure 2b. Potassium was left from the process of MnO_2 precipitation, while iron was the catalyst for carbon nanotube growth. Figure 2c shows the typical X-ray diffraction (XRD) pattern of MnO_2 nanoparticles precipitated from $KMnO_4$. The four characteristic peaks at 12°, 24°, 37°, and 66° can be indexed to birnessite-type MnO_2.[42,54,55] Broad peaks are related to the nanostructure of the MnO_2 powder.

To identify the potential window of asymmetric supercapacitor and balance the charges between positive and negative electrodes, the electrochemical performance of the MnO_2/CNT hybrid fiber electrode and pristine aerogel CNT fiber electrode was investigated in a three-electrode system using platinum foil, Ag/AgCl, and 1 M KOH aqueous solution as the counter electrode, reference electrode, and electrolyte, respectively. MnO_2/CNT hybrid fiber electrode showed a stable potential window in the range of 0−0.5 V, while the pristine CNT fiber electrode exhibited the stable potential window of −1.0 − −0.4 V, indicating that the potential window of the assembled asymmetric supercapacitor can be extended to 1.5 V as shown in Figure 3a. At the scan rate of 100 mV s^{-1}, the specific capacitances of MnO_2/CNT hybrid fiber positive electrode and pristine CNT fiber negative electrode were 90.4 and 30.5 mF cm^{-2}, respectively. The surface area (S) of the electrode was calculated according to the equation $S = \pi dL$, where d is the diameter of the fiber electrode and L is the length of the fiber immersed in the gel electrolyte. The galvanostatic charge−discharge curves of positive and negative electrodes at current densities ranging from 2 to 10 mA cm^{-2} were shown in Figure 3, panels b and c, respectively.

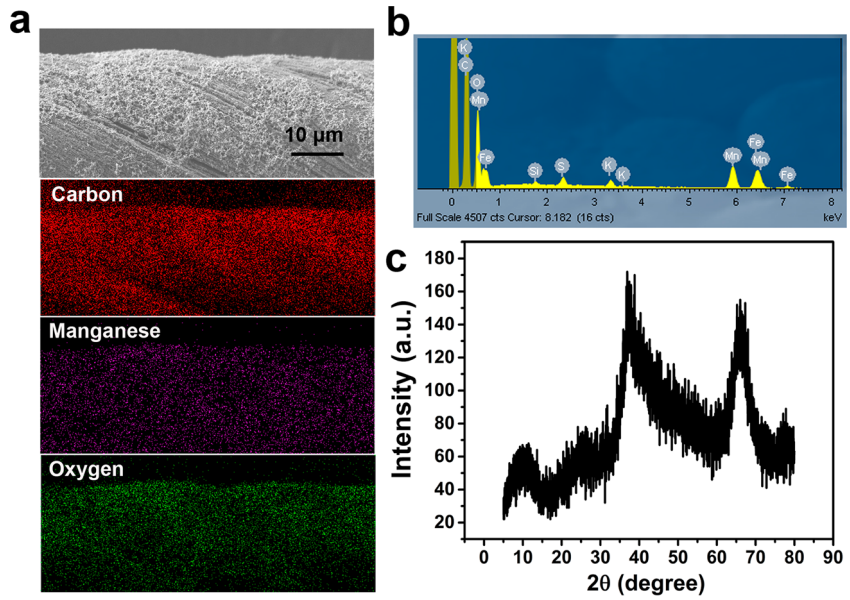

Figure 2. Positive electrode characterization. (a) Energy-dispersive X-ray (EDX) mappings of carbon, manganese, and oxygen elements on the surface of MnO_2/CNT hybrid fiber. (b) EDX spectrum. (c) XRD pattern of MnO_2/CNT hybrid fiber.

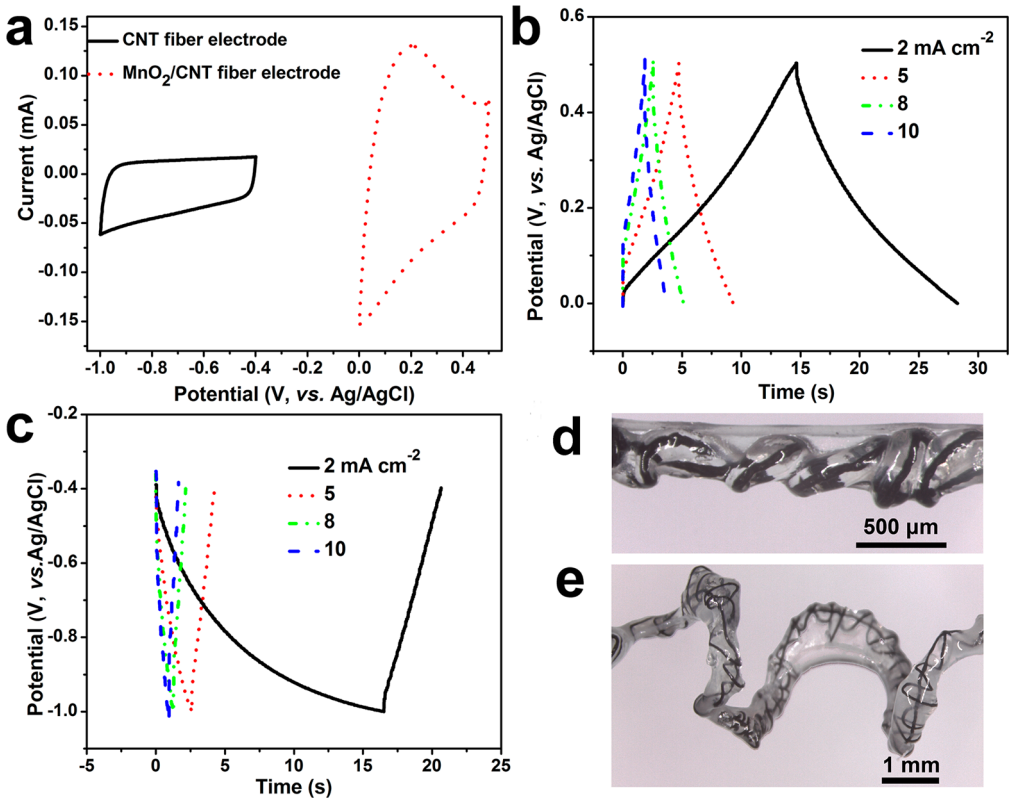

Figure 3. (a) Comparative CV curves of MnO_2/CNT hybrid fiber and pristine CNT fiber electrodes obtained in a three-electrode system in 1 M KOH aqueous solution at a scan rate of 100 mV s^{-1}. Galvanostatic charge–discharge curves of (b) positive and (c) negative electrodes at different current densities. Optical images of (d) straight asymmetric supercapacitor adhered to the Dow XLA elastic fiber and (e) buckled stretchable asymmetric supercapacitor.

The charge balance between the two electrodes follows the relationship $q_+ = q_-$, in which the stored charge by each electrode is determined by the specific capacitance (C), the potential range for the charge/discharge process (ΔE), and the surface area of each electrode (S) using the following relation.[42,44]

$$q = C \times \Delta E \times S$$

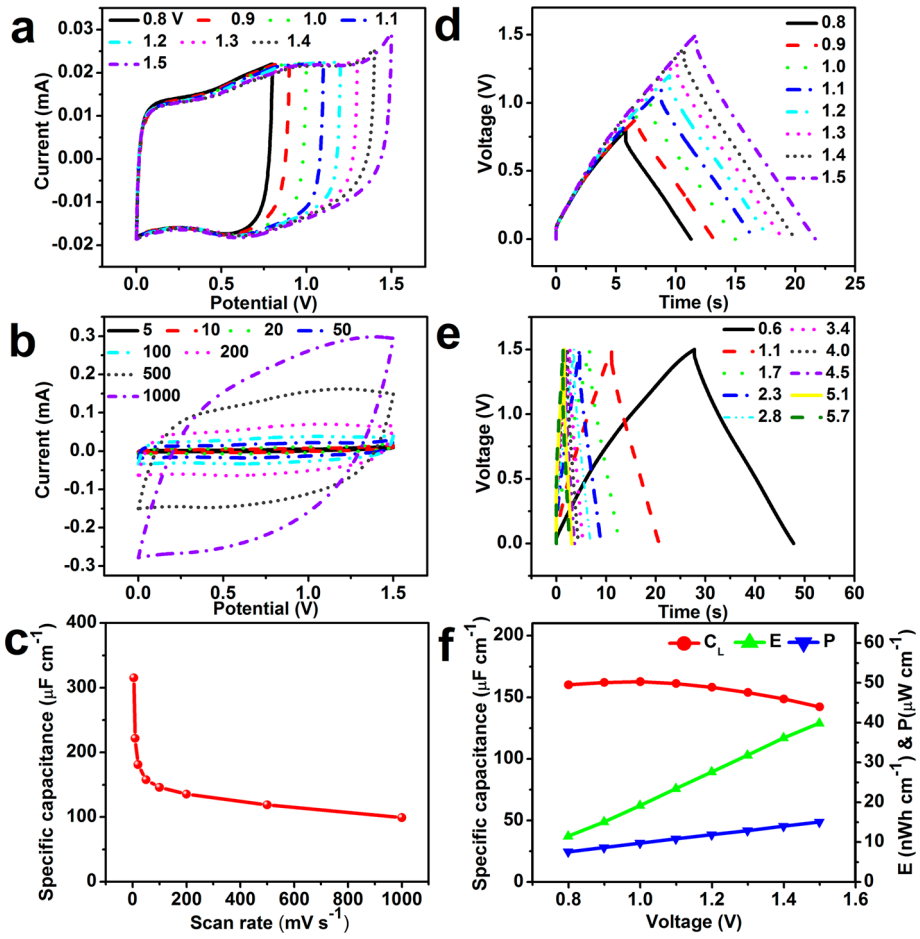

Figure 4. Electrochemical performance of straight asymmetric supercapacitor. (a) CV curves tested over different voltages from 0.8 to 1.5 V. (b) CV curves of an optimized asymmetric supercapacitor at scan rates ranging from 5 to 1000 mV s^{-1}. (c) Specific capacitance variation with scan rate. (d) Galvanostatic charge−discharge curves obtained over different voltages from 0.8 to 1.5 V at a current density of 1.1 mA cm^{-2}. (e) Galvanostatic charge−discharge curves at different current densities from 0.6 to 5.7 mA cm^{-2} in the potential window of 1.5 V. (f) Effects of extended potential window on specific capacitance (C_L), energy density (E), and power density (P).

On the basis of the calculation, the optimal length ratio between the two electrodes should be $L_{\_MnO2/CNTF}/L_{\_CNTF} = 0.37$.

To fabricate the asymmetric supercapacitor, the MnO_2/CNT hybrid fiber, pristine CNT fiber, and KOH-PVA gel electrolyte (around 0.81 M) were used as the positive electrode, negative electrode, and electrolyte, respectively. To keep charges balanced on both positive and negative electrodes, the gel electrolyte was coated over the pristine CNT fiber and MnO_2/CNT hybrid fiber along the lengths of 5.5 and 2 cm, respectively. Note that 2 cm/5.5 cm was slightly lower than the optimal length ratio of 0.37, and these lengths were used to ensure the pseudocapacitive material MnO_2 to be thoroughly utilized. Furthermore, in order to fully take advantage of the counterpart areas of positive and negative electrodes, the gel-electrolyte-coated pristine CNT fiber was wound around the electrolyte-coated MnO_2/CNT hybrid fiber to form the asymmetric supercapacitor. Then, the supercapacitor was made stretchable by applying the simple prestrainning-then-buckling strategy. More specifically, the WSS was attached onto the gel-electrolyte-coated elastic fiber with the prestrain of 100%, taking advantage of the stickiness of gel electrolyte. The WSS became buckled and stretchable with stretchability of up to 100% upon releasing the elastic fiber.[32] The digital photos of the straight and buckled asymmetric supercapacitors are shown in Figure 3, panels d and e, respectively.

CV curves at 50 mV s^{-1} and galvanostatic charge−discharge curves at 1.1 mA cm^{-2} of the asymmetric supercapacitor at different potential windows in KOH-PVA gel electrolyte are displayed in Figure 4, panels a and d, respectively. Even when the potential window was increased up to 1.5 V, the rectangular shape of the CV curves with two weak symmetric broad redox peaks and symmetric triangular shape of the charge−discharge curves were maintained, indicating a good capacitive behavior. The weak broad redox peaks were attributed to the pseudocapacitive property of the supercapacitor resulted from the Faradaic reaction of MnO_2.

The CV curves and charge−discharge curves in the extended potential window of 1.5 V were further investigated at different scan rates and current densities,

TABLE 1. Comparison of Specific Capacitances of WSSs

electrode materials	C_A (mF cm^{-2})	C_L (μF cm^{-1})	C_V (F cm^{-3})	characterization conditions
MnO_2/CNT fiber and CNT fiber-straight	10.61—23.74	99.06—221.67	13.34—29.85	CV[a]: 10—1000 mV s^{-1}
	13.89—15.85	129.90—148.16	17.49—19.95	GCD[b]: 0.6—5.7 mA cm^{-2}
MnO_2/CNT fiber and CNT fiber-stretchable	8.82—27.98	82.35—261.29	11.09—35.19	CV: 10—1000 mV s^{-1}
	12.11—16.82	113.21—157.29	15.25—21.18	GCD: 0.6—5.7 mA cm^{-2}
MnO_2/graphene/graphene fiber[21]	9.1—9.6	-	-	GCD: 2 μA
ZnO nanowire/polymer fiber[20]	2.4	-	-	CV: 100 mV s^{-1}
All-graphene core—shell microfibers[29]	1.2—1.7	20	-	GCD: 17—424.6 μA cm^{-2}
TiO_2 nanotubes on wire and CNT fiber[22]	0.6	24	-	GCD: 0.25 μA
TiO_2 nanotubes on wire and CNT sheet[57]	3.32	156	-	GCD: 1 μA
CNT/polyaniline nanowire hybrid fiber[31]	12	-	-	GCD: 1 mA cm^{-2}
Pen ink coated polymer fiber[25]	9.5	-	-	CV: 1000 mV s^{-1}
MWCNT/MnO_2 composite fiber[30]	3.16—3.57	16—19	-	GCD: 0.5—10 μA
Graphene/CNT composite fiber[59]	4.97	27.1	-	GCD: 0.04 A g^{-1}
CNT fiber springs[39]	27.07	510	12.25—18.12	GCD: 150 mA cm^{-3}
CNT fiber, CNT film[24]	8.66	29	32.09	GCD: 1 μA
Reduced graphene oxide on Au wire[28]	6.49	107.9	-	GCD: 2.5 μA cm^{-1}
CNT fiber[32]	4.63—4.99	12.3—13.3	-	CV: 50 mV s^{-1}
PANI/Stainless steel[26]	19	-	-	GCD: 0.32—12.8 mA cm^{-2}

[a] Cyclic voltammograms (CV). [b] Galvanostatic charge—discharge test (GCD).

as shown in Figure 4, panels b and e, respectively. Due to the difficulty of measuring the accurate weight of active materials in microsupercapacitors, the areal capacitance (C_A, mF cm^{-2}), volumetric capacitance (C_V, F cm^{-3}), and length specific capacitance (C_L, μF cm^{-1}) are more suitable than the gravimetric capacitance to evaluate the capacitance for WSS,[56] which were all presented for comparison. The areal and volumetric capacitance were derived from the average surface area and volume of both electrodes. At scan rate of 50 mV s^{-1}, the length specific capacitance was 157.53 μF cm^{-1}, with corresponding areal specific capacitance and volumetric capacitance of 16.87 mF cm^{-2} and 21.21 F cm^{-3}, respectively. Thus, the areal specific capacitance and volumetric capacitance were around 4 times and over 1.8 times, respectively, the values reported in our previous study on symmetric stretchable WSS.[32] The volumetric capacitance was higher than that of WSS composed by carbon nanotube fiber springs (12.25—18.12 F cm^{-3}).[39] Due to the insufficient time for the ions to approach the electrodes at high scan rates,[58] the length specific capacitance decreased from 315.17 (C_A, 33.75 mF cm^{-2}; C_V, 42.45 F cm^{-3}) to 99.06 μF cm^{-1} (C_A, 10.61 mF cm^{-2}; C_V, 13.34 F cm^{-3}) as the scan rate increased from 5 to 1000 mV s^{-1} in Figure 4c. Notably, the areal, length and volumetric specific capacitances of the stretchable asymmetric WSS were comparable or even exceeded those of many previously reported WSS without stretchability exhibited in Table 1. With the volumetric ratio of the active materials including the pristine CNT fiber and MnO_2/CNT hybrid fiber around 2.7%, the device volumetric capacitance of the stretchable asymmetric WSS, which also took the volumes of gel electrolyte and elastic fiber into account, varied from 75.02 to 238.01 mF cm^{-3} as the scan rate varied in the range of 10—1000 mV s^{-1}. According to calculations based on Figure 4d, the effects of extending potential window on specific capacitance, energy density and power density are depicted in Figure 4f. Although the specific capacitance started to decline slightly from 162.63 μF cm^{-1} at 1 V to 142.22 μF cm^{-1} at 1.5 V, the energy density rose linearly and tripled from 11.47 to 39.85 nWh cm^{-1}, and the corresponding power density doubled from 7.59 to 15.03 μW cm^{-1} as the potential window extended from 0.8 to 1.5 V.

To demonstrate the stretchability of the asymmetric WSS, CV curves and galvanostatic charge—discharge curves were measured at applied tensile strains of 0%, 40%, 70%, and 100% and after 20 mechanical stretching-releasing cycles (MSRCs) (Figure 5). Figure 5a exhibited the CV curves of the asymmetric supercapacitor after 20 MSRCs. At the scan rate of up to 500 mV s^{-1}, the CV curve still maintained the symmetric rectangular shape, indicating that the asymmetric supercapacitor possessed not only excellent electrochemical performance but also superb mechanical robustness. At different stretching states, CV curves in Figure 5b did not show substantial changes and maintained the redox peaks. The curves in Figure 5c, which displayed the specific capacitances as functions of scan rates, only varied in a small range. The slopes of discharge curves in Figure 5d maintained approximately constant as the supercapacitor deformed at different tensile strains (0%, 40%, 70%, and 100%) and after 20 MSRCs, indicating small capacitance change. The Ragone plots in Figure 5e compared the energy densities and power densities of the stretchable WSS at all stretching levels. Note that instead of using the electrode capacitance (C_+ or C_-), cell capacitance C_{cell} ($1/C_{cell} = 1/C_+ + 1/C_-$) should be used to calculate the energy density. Thus, the energy density of the CNT fiber

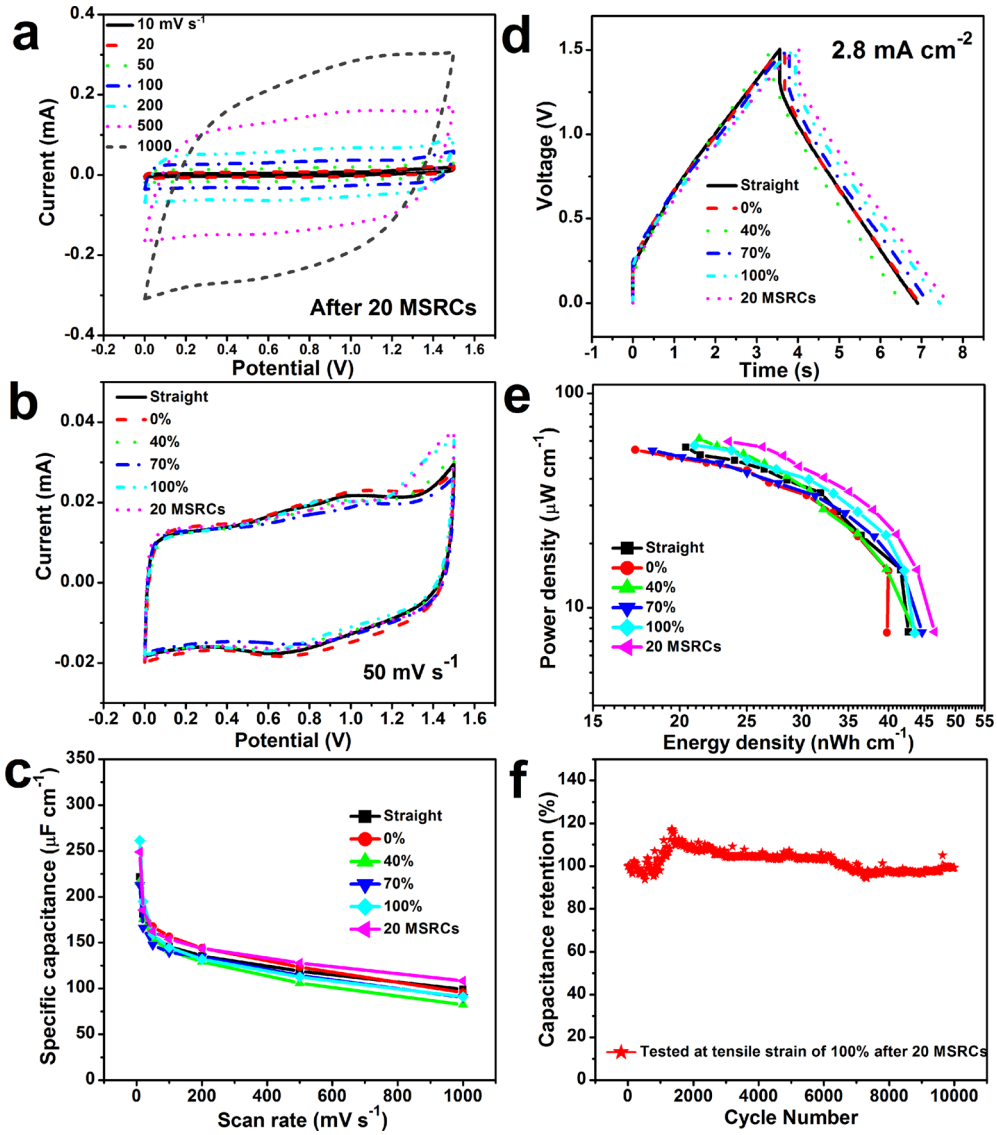

Figure 5. Electrochemical performance of the stretchable asymmetric WSS. (a) CV curves obtained at different scan rates after the supercapacitor was subject to 20 MSRCs. (b) CV curves at different stretching states. (c) Specific capacitance variations with scan rates. (d) Galvanostatic charge–discharge curves of asymmetric supercapacitor at different tensile strains. (e) Ragone plots of the supercapacitor at different stretching states. (f) Cycling performance of the asymmetric supercapacitor at current density of 2.8 mA cm^{-2} after 20 MSRCs.

based symmetric stretchable supercapacitor in our previous paper (ref 32) should be half of the reported value, namely, 0.0465–0.144 μWh cm^{-2}. Due to the extended potential window and enhanced specific capacitance, the areal specific energy density of the straight asymmetric WSS was around 9 times larger than that of stretchable symmetric WSS,[32] varying from 0.55 to 1.14 μWh cm^{-2} (length specific energy density from 20.43 to 42.73 nWh cm^{-1}, volumetric energy density from 0.69 to 1.44 mWh cm^{-3}) in the areal specific power density range of 0.21–1.50 mW cm^{-2} (length specific power density, 7.70–56.16 μW cm^{-1}; volumetric power density, 0.26–1.89 W cm^{-3}). Under the stretched states, the asymmetric WSS also had a similar enhanced performance: the energy density was in the range of 17.26–46.59 nWh cm^{-1} (or 0.46–1.25 μWh cm^{-2} and 0.58–1.57 mWh cm^{-3}) and the power density varied from 7.63 to 61.55 μW cm^{-1} (or from 0.20 to 1.65 mW cm^{-2} and from 0.26 to 2.08 W cm^{-3}). The areal specific energy density (E_A) and power density (P_A) of the stretchable asymmetric WSS also surpassed the supercapacitors based on ZnO nanowires coated polymer fiber (E_A = 0.027 μWh cm^{-2}, P_A = 0.014 mW cm^{-2}),[20] and all-graphene core–shell microfiber (E_A = 0.04–0.17 μWh cm^{-2}, P_A = 0.006–0.1 mW cm^{-2}).[29] The maximum volumetric energy density (E_V = 1.57 mWh cm^{-3}) and power density (P_V = 2.08 W cm^{-3}) of the stretchable supercapacitor were much higher than those of stretchable CNT fiber spring based supercapacitor (E_V = 0.629 mWh cm^{-3}, P_V = 0.03774 W cm^{-3}),[39] and comparable to WSS derived from MWCNT/MnO_2 composite fiber (E_V = 1.73 mWh cm^{-3}, P_V = 0.79 W cm^{-3}).[30]

In addition, based on the whole volume of the stretchable asymmetric WSS, the energy densities were in the range of 15.73−42.44 μWh cm^{-3} corresponding to power densities in the range of 6.95−56.06 mW cm^{-3}. After 20 MSRCs, the supercapacitor capacitance retention was recorded at tensile strain of 100%. As shown in Figure 5f, the capacitance maintained at more than 99% over 10 000 charge−discharge cycles, indicating a good electrochemical cyclability. Their high specific capacitance, high energy density, high power density and good cyclability confirmed that this asymmetric supercapacitor achieved the advantages of both batteries and supercapacitors.

This stretchable asymmetric WSS has the potential to be attached onto various textiles and manually woven or knitted into textiles, like some previous reported work.[11,14,19,27,31] As for the formation of textiles by machine weaving or knitting demonstrated in ref 60, different fabric structures and different processing parameters would exert different levels of tensions and could be systematically investigated to ensure the intactness of the stretchable supercapacitor during processing in the future research. Technically, the stretchable or flexible properties of the supercapacitor resulting from the excellent flexibility of CNT fiber, MnO_2/CNT fiber and elastic fiber enable the supercapacitor to tolerate certain tension through deformation.

CONCLUSIONS

In conclusion, a stretchable asymmetric wire-shaped supercapacitor composed of MnO_2/CNT hybrid fiber positive electrode, pristine CNT fiber negative electrode and KOH-PVA gel electrolyte was fabricated. Due to the good conductivity of the aerogel CNT fiber and the extended potential window, the specific capacitance and the energy density were greatly enhanced. In addition to the excellent electrochemical performance, the remarkable stretchability of up to 100% tensile strain made this supercapacitor a promising energy storage device for smart textiles. The simplistic fabrication procedures, including anchoring MnO_2 on CNT fiber at room temperature and making the asymmetric wire-shaped supercapacitor stretchable by prestrainning-then-buckling method, are suitable for scalable fabrication. The asymmetric configuration has been demonstrated to be the preferable supercapacitor structure to achieve higher operating voltage and high energy without sacrificing the power delivery and cycle stability.

EXPERIMENTAL SECTION

MnO_2 Precipitation. The pristine CNT fiber was spun with CNT aerogel[38] at the Suzhou Institute of Nano-Tech and Nano-Bionics. To fabricate the MnO_2/CNT hybrid fiber positive electrode, the aerogel CNT fibers were immersed in ethanol, and 0.75 mL of 0.1 M $KMnO_4$ aqueous solution was added. After nearly 40 min, the intense purple color disappeared and brownish precipitates were formed and anchored on the surface of CNT fiber, suggesting that MnO_4^- was reduced by ethanol into MnO_2.[50−53]

Gel Electrolyte Preparation. The KOH-PVA gel electrolyte was prepared by mixing KOH (3 g) with deionized water (60 mL), and then adding PVA powder (6 g, Sigma-Aldrich, Mw = 89 000−98 000). The solution was subjected to vigorous stirring throughout the mixing process and the subsequent heating to 85 °C until the solution became clear.

Supercapacitor Fabrication. The pristine aerogel CNT fiber and the MnO_2/CNT hybrid fiber were coated with the liquid KOH-PVA gel electrolyte by means of dip-coating and subsequently twisted together to form the WSS. Then, a thin layer of gel electrolyte was applied again on the outside of the twisted fibers. While the two fibers were being twisted together, the electrical resistance between them was monitored by a multimeter to detect any short-circuit.

Performance Characterization. The surface morphology of the CNT fibers was characterized by scanning electron microscopy (SEM, JEOL, JSM-7400F operated at 3 kV). The energy-dispersive X-ray analysis (EDX) was obtained on a JSM-7400F SEM unit. X-ray diffraction pattern of MnO_2 powder was recorded by Philips X'Pert diffractometer with Cu Kα radiation in the 2θ range of 5°−80° at 0.02° step^{-1} and 1 s step^{-1}. The electrochemical performance of the WSS was investigated by cyclic voltammograms (CV) and galvanostatic charge−discharge cycling using a PARSTAT 2273 potentiostat/galvonostat Advanced Electrochemical System (Princeton Applied Research) and an Arbin Potentiostat test system.

Conflict of Interest: The authors declare no competing financial interest.

Acknowledgment. T.-W. Chou thanks the support of the National Research Foundation of Korea through the Korean Ministry for Education, Science and Technology (MEST). P. Xu's study abroad at the University of Delaware was supported by the State Scholarship Fund of the China Scholarship Council as well as Doctorial Innovation Fund of Donghua University. Funding by National Research Foundation of Korea through the Korean Ministry for Education, Science and Technology (MEST) State Scholarship Fund of the China Scholarship Council Doctorial Innovation Fund of Donghua University. T.-W.C and J.Y. supervised the research work. P.X conducted the experiments and drafted the manuscript. Z.C. performed the XRD experiment and offered helpful discussion. B.W, J.Z., K.G., F.L., Q.L, W.L., J.-H.B., B.-S.K. and Y.Y provided valuable advice.

REFERENCES AND NOTES

1. Jost, K.; Stenger, D.; Perez, C. R.; McDonough, J. K.; Lian, K.; Gogotsi, Y.; Dion, G. Knitted and Screen Printed Carbon-Fiber Supercapacitors for Applications in Wearable Electronics. *Energy Environ. Sci.* **2013**, *6*, 2698–2705.
2. Xie, K.; Wei, B. Materials and Structures for Stretchable Energy Storage and Conversion Devices. *Adv. Mater.* **2014**, *26*, 3592–3617.
3. Jost, K.; Dion, G.; Gogotsi, Y. Textile Energy Storage in Perspective. *J. Mater. Chem. A* **2014**, *2*, 10776–10787.
4. Cai, X.; Peng, M.; Yu, X.; Fu, Y.; Zou, D. Flexible Planar/Fiber-Architectured Supercapacitors for Wearable Energy Storage. *J. Mater. Chem. C* **2014**, *2*, 1184–1200.
5. Bao, L.; Li, X. Towards Textile Energy Storage from Cotton T-Shirts. *Adv. Mater.* **2012**, *24*, 3246–3252.
6. Hu, L.; Pasta, M.; Mantia, F. L.; Cui, L.; Jeong, S.; Deshazer, H. D.; Choi, J. W.; Han, S. M.; Cui, Y. Stretchable, Porous, and Conductive Energy Textiles. *Nano Lett.* **2010**, *10*, 708–714.
7. Pasta, M.; La Mantia, F.; Hu, L.; Deshazer, H.; Cui, Y. Aqueous Supercapacitors on Conductive Cotton. *Nano Res.* **2010**, *3*, 452–458.
8. Yun, Y. J.; Hong, W. G.; Kim, W.-J.; Jun, Y.; Kim, B. H. A Novel Method for Applying Reduced Graphene Oxide Directly to

Electronic Textiles from Yarns to Fabrics. *Adv. Mater.* **2013**, *25*, 5701–5705.
9. Liu, W.-W.; Yan, X.-B.; Lang, J.-W.; Peng, C.; Xue, Q.-J. Flexible and Conductive Nanocomposite Electrode Based on Graphene Sheets and Cotton Cloth for Supercapacitor. *J. Mater. Chem.* **2012**, *22*, 17245–17253.
10. Bae, J.; Park, Y. J.; Lee, M.; Cha, S. N.; Choi, Y. J.; Lee, C. S.; Kim, J. M.; Wang, Z. L. Single-Fiber-Based Hybridization of Energy Converters and Storage Units Using Graphene as Electrodes. *Adv. Mater.* **2011**, *23*, 3446–3449.
11. Cai, Z.; Li, L.; Ren, J.; Qiu, L.; Lin, H.; Peng, H. Flexible, Weavable and Efficient Microsupercapacitor Wires Based on Polyaniline Composite Fibers Incorporated With Aligned Carbon Nanotubes. *J. Mater. Chem. A* **2013**, *1*, 258–261.
12. Cao, Y.; Zhu, M.; Li, P.; Zhang, R.; Li, X.; Gong, Q.; Wang, K.; Zhong, M.; Wu, D.; Lin, F.; et al. Boosting Supercapacitor Performance of Carbon Fibres Using Electrochemically Reduced Graphene Oxide Additives. *Phys. Chem. Chem. Phys.* **2013**, *15*, 19550–19556.
13. Cheng, H.; Dong, Z.; Hu, C.; Zhao, Y.; Hu, Y.; Qu, L.; Chen, N.; Dai, L. Textile Electrodes Woven by Carbon Nanotube-Graphene Hybrid Fibers for Flexible Electrochemical Capacitors. *Nanoscale* **2013**, *5*, 3428–3434.
14. Choi, C.; Lee, J. A.; Choi, A. Y.; Kim, Y. T.; Lepró, X.; Lima, M. D.; Baughman, R. H.; Kim, S. J. Flexible Supercapacitor Made of Carbon Nanotube Yarn with Internal Pores. *Adv. Mater.* **2014**, *26*, 2059–2065.
15. Dalton, A. B.; Collins, S.; Munoz, E.; Razal, J. M.; Ebron, V. H.; Ferraris, J. P.; Coleman, J. N.; Kim, B. G.; Baughman, R. H. Super-Tough Carbon-Nanotube Fibres. *Nature* **2003**, *423*, 703–703.
16. Le, V. T.; Kim, H.; Ghosh, A.; Kim, J.; Chang, J.; Vu, Q. A.; Pham, D. T.; Lee, J.-H.; Kim, S.-W.; Lee, Y. H. Coaxial Fiber Supercapacitor Using All-Carbon Material Electrodes. *ACS Nano* **2013**, *7*, 5940–5947.
17. Lin, H.; Weng, W.; Ren, J.; Qiu, L.; Zhang, Z.; Chen, P.; Chen, X.; Deng, J.; Wang, Y.; Peng, H. Twisted Aligned Carbon Nanotube/Silicon Composite Fiber Anode for Flexible Wire-Shaped Lithium-Ion Battery. *Adv. Mater.* **2014**, *26*, 1217–1222.
18. Ren, J.; Bai, W.; Guan, G.; Zhang, Y.; Peng, H. Flexible and Weaveable Capacitor Wire Based on a Carbon Nanocomposite Fiber. *Adv. Mater.* **2013**, *25*, 5965–5970.
19. Zhang, Z.; Chen, X.; Chen, P.; Guan, G.; Qiu, L.; Lin, H.; Yang, Z.; Bai, W.; Luo, Y.; Peng, H. Integrated Polymer Solar Cell and Electrochemical Supercapacitor in a Flexible and Stable Fiber Format. *Adv. Mater.* **2014**, *26*, 466–470.
20. Bae, J.; Song, M. K.; Park, Y. J.; Kim, J. M.; Liu, M.; Wang, Z. L. Fiber Supercapacitors Made of Nanowire-Fiber Hybrid Structures for Wearable/Flexible Energy Storage. *Angew. Chem., Int. Ed.* **2011**, *50*, 1683–1687.
21. Chen, Q.; Meng, Y.; Hu, C.; Zhao, Y.; Shao, H.; Chen, N.; Qu, L. MnO_2-Modified Hierarchical Graphene Fiber Electrochemical Supercapacitor. *J. Power Sources* **2014**, *247*, 32–39.
22. Chen, T.; Qiu, L.; Yang, Z.; Cai, Z.; Ren, J.; Li, H.; Lin, H.; Sun, X.; Peng, H. An Integrated "Energy Wire" for Both Photoelectric Conversion and Energy Storage. *Angew. Chem., Int. Ed.* **2012**, *51*, 11977–11980.
23. Chen, T.; Yang, Z.; Peng, H. Integrated Devices to Realize Energy Conversion and Storage Simultaneously. *ChemPhysChem* **2013**, *14*, 1777–1782.
24. Chen, X.; Qiu, L.; Ren, J.; Guan, G.; Lin, H.; Zhang, Z.; Chen, P.; Wang, Y.; Peng, H. Novel Electric Double-Layer Capacitor With a Coaxial Fiber Structure. *Adv. Mater.* **2013**, *25*, 6436–6441.
25. Fu, Y.; Cai, X.; Wu, H.; Lv, Z.; Hou, S.; Peng, M.; Yu, X.; Zou, D. Fiber Supercapacitors Utilizing Pen Ink for Flexible/Wearable Energy Storage. *Adv. Mater.* **2012**, *24*, 5713–5718.
26. Fu, Y.; Wu, H.; Ye, S.; Cai, X.; Yu, X.; Hou, S.; Kafafy, H.; Zou, D. Integrated Power Fiber for Energy Conversion and Storage. *Energy Environ. Sci.* **2013**, *6*, 805–812.
27. Lee, J. A.; Shin, M. K.; Kim, S. H.; Cho, H. U.; Spinks, G. M.; Wallace, G. G.; Lima, M. D.; Lepró, X.; Kozlov, M. E.; Baughman, R. H.; et al. Ultrafast Charge and Discharge Biscrolled Yarn Supercapacitors for Textiles and Microdevices. *Nat. Commun.* **2013**, *4*, 1970.
28. Li, Y.; Sheng, K.; Yuan, W.; Shi, G. A High-Performance Flexible Fibre-Shaped Electrochemical Capacitor Based on Electrochemically Reduced Graphene Oxide. *Chem. Commun.* **2013**, *49*, 291–293.
29. Meng, Y.; Zhao, Y.; Hu, C.; Cheng, H.; Hu, Y.; Zhang, Z.; Shi, G.; Qu, L. All-Graphene Core-Sheath Microfibers for All-Solid-State, Stretchable Fibriform Supercapacitors and Wearable Electronic Textiles. *Adv. Mater.* **2013**, *25*, 2326–2331.
30. Ren, J.; Li, L.; Chen, C.; Chen, X.; Cai, Z.; Qiu, L.; Wang, Y.; Zhu, X.; Peng, H. Twisting Carbon Nanotube Fibers for Both Wire-Shaped Micro-Supercapacitor and Micro-Battery. *Adv. Mater.* **2013**, *25*, 1155–1159.
31. Wang, K.; Meng, Q.; Zhang, Y.; Wei, Z.; Miao, M. High-Performance Two-Ply Yarn Supercapacitors Based on Carbon Nanotubes and Polyaniline Nanowire Arrays. *Adv. Mater.* **2013**, *25*, 1494–1498.
32. Xu, P.; Gu, T.; Cao, Z.; Wei, B.; Yu, J.; Li, F.; Byun, J.-H.; Lu, W.; Li, Q.; Chou, T.-W. Carbon Nanotube Fiber Based Stretchable Wire-Shaped Supercapacitors. *Adv. Energy Mater.* **2013**, *4*, 1300759.
33. Yang, Z.; Deng, J.; Chen, X.; Ren, J.; Peng, H. A Highly Stretchable, Fiber-Shaped Supercapacitor. *Angew. Chem., Int. Ed.* **2013**, *52*, 13453–13457.
34. Benight, S. J.; Wang, C.; Tok, J. B. H.; Bao, Z. Stretchable and Self-Healing Polymers and Devices for Electronic Skin. *Prog. Polym. Sci.* **2013**, *38*, 1961–1977.
35. White, M. S.; Kaltenbrunner, M.; Glowacki, E. D.; Gutnichenko, K.; Kettlgruber, G.; Graz, I.; Aazou, S.; Ulbricht, C.; Egbe, D. A. M.; Miron, M. C.; et al. Ultrathin, Highly Flexible and Stretchable PLEDs. *Nat. Photonics* **2013**, *7*, 811–816.
36. Chou, T.-W.; Gao, L.; Thostenson, E. T.; Zhang, Z.; Byun, J.-H. An Assessment of the Science and Technology of Carbon Nanotube-Based Fibers and Composites. *Compos. Sci. Technol.* **2010**, *70*, 1–19.
37. Wu, A. S.; Chou, T.-W. Carbon Nanotube Fibers for Advanced Composites. *Mater. Today* **2012**, *15*, 302–310.
38. Lu, W.; Zu, M.; Byun, J.-H.; Kim, B.-S.; Chou, T.-W. State of the Art of Carbon Nanotube Fibers: Opportunities and Challenges. *Adv. Mater.* **2012**, *24*, 1805–1833.
39. Zhang, Y.; Bai, W.; Cheng, X.; Ren, J.; Weng, W.; Chen, P.; Fang, X.; Zhang, Z.; Peng, H. Flexible and Stretchable Lithium-Ion Batteries and Supercapacitors Based on Electrically Conducting Carbon Nanotube Fiber Springs. *Angew. Chem., Int. Ed.* **2014**, *53*, 14564–14568.
40. Chen, T.; Hao, R.; Peng, H.; Dai, L. High-Performance, Stretchable, Wire-Shaped Supercapacitors. *Angew. Chem., Int. Ed.* **2015**, *54*, 618–622.
41. Wang, X.; Liu, B.; Liu, R.; Wang, Q.; Hou, X.; Chen, D.; Wang, R.; Shen, G. Fiber-Based Flexible All-Solid-State Asymmetric Supercapacitors for Integrated Photodetecting System. *Angew. Chem., Int. Ed.* **2014**, *53*, 1849–1853.
42. Fan, Z.; Yan, J.; Wei, T.; Zhi, L.; Ning, G.; Li, T.; Wei, F. Asymmetric Supercapacitors Based on Graphene/MnO_2 and Activated Carbon Nanofiber Electrodes with High Power and Energy Density. *Adv. Funct. Mater.* **2011**, *21*, 2366–2375.
43. Zhang, Z.; Xiao, F.; Qian, L.; Xiao, J.; Wang, S.; Liu, Y. Facile Synthesis of 3D MnO_2—Graphene and Carbon Nanotube—Graphene Composite Networks for High-Performance, Flexible, All-Solid-State Asymmetric Supercapacitors. *Adv. Energy Mater.* **2014**, *4*, 1400064.
44. Yan, J.; Fan, Z.; Sun, W.; Ning, G.; Wei, T.; Zhang, Q.; Zhang, R.; Zhi, L.; Wei, F. Advanced Asymmetric Supercapacitors Based on $Ni(OH)_2$/Graphene and Porous Graphene Electrodes with High Energy Density. *Adv. Funct. Mater.* **2012**, *22*, 2632–2641.
45. Yu, D. S.; Goh, K. L.; Zhang, Q.; Wei, L.; Wang, H.; Jiang, W. C.; Chen, Y. Controlled Functionalization of Carbonaceous Fibers for Asymmetric Solid-State Micro-Supercapacitors with High Volumetric Energy Density. *Adv. Mater.* **2014**, *26*, 6790–6797.

46. Dong, X.; Guo, Z.; Song, Y.; Hou, M.; Wang, J.; Wang, Y.; Xia, Y. Flexible and Wire-Shaped Micro-Supercapacitor Based on $Ni(OH)_2$-Nanowire and Ordered Mesoporous Carbon Electrodes. *Adv. Funct. Mater.* **2014**, *24*, 3405–3412.
47. Su, F.; Miao, M. Asymmetric Carbon Nanotube−MnO_2 Two-Ply Yarn Supercapacitors for Wearable Electronics. *Nanotechnology* **2014**, *25*, 135401.
48. Wang, G. P.; Zhang, L.; Zhang, J. J. A Review of Electrode Materials for Electrochemical Supercapacitors. *Chem. Soc. Rev.* **2012**, *41*, 797–828.
49. Wei, W. F.; Cui, X. W.; Chen, W. X.; Ivey, D. G. Manganese Oxide-Based Materials As Electrochemical Supercapacitor Electrodes. *Chem. Soc. Rev.* **2011**, *40*, 1697–1721.
50. Subramanian, V.; Zhu, H. W.; Wei, B. Q. Alcohol-Assisted Room Temperature Synthesis of Different Nanostructured Manganese Oxides and Their Pseudocapacitance Properties in Neutral Electrolyte. *Chem. Phys. Lett.* **2008**, *453*, 242–249.
51. Subramanian, V.; Zhu, H. W.; Wei, B. Q. Nanostructured Manganese Oxides and Their Composites with Carbon Nanotubes as Electrode Materials for Energy Storage Devices. *Pure Appl. Chem.* **2008**, *80*, 2327–2343.
52. Li, X.; Wei, B. Q. Facile Synthesis and Super Capacitive Behavior of SWNT/MnO_2 Hybrid Films. *Nano Energy* **2012**, *1*, 479–487.
53. Li, X. M.; Zhao, T. S.; Chen, Q.; Li, P. X.; Wang, K. L.; Zhong, M. L.; Wei, J. Q.; Wu, D. H.; Wei, B. Q.; Zhu, H. W. Flexible All Solid-State Supercapacitors Based on Chemical Vapor Deposition Derived Graphene Fibers. *Phys. Chem. Chem. Phys.* **2013**, *15*, 17752–17757.
54. Ma, S.-B.; Ahn, K.-Y.; Lee, E.-S.; Oh, K.-H.; Kim, K.-B. Synthesis and Characterization of Manganese Dioxide Spontaneously Coated on Carbon Nanotubes. *Carbon* **2007**, *45*, 375–382.
55. Julien, C. M.; Poinsignon, C. Lattice Vibrations of Manganese Oxides: Part I. Periodic Structures. *Spectrochim. Acta, Part A* **2004**, *60*, 689–700.
56. Kou, L.; Huang, T.; Zheng, B.; Han, Y.; Zhao, X.; Gopalsamy, K.; Sun, H.; Gao, C. Coaxial Wet-Spun Yarn Supercapacitors for High-Energy Density and Safe Wearable Electronics. *Nat. Commun.* **2014**, *5*, 3754.
57. Chen, X.; Sun, H.; Yang, Z.; Guan, G.; Zhang, Z.; Qiu, L.; Peng, H. A Novel "Energy Fiber" by Coaxially Integrating Dye-Sensitized Solar Cell and Electrochemical Capacitor. *J. Mater. Chem. A* **2014**, *2*, 1897–1902.
58. Niu, Z.; Zhang, L.; Liu, L.; Zhu, B.; Dong, H.; Chen, X. All-Solid-State Flexible Ultrathin Micro-Supercapacitors Based on Graphene. *Adv. Mater.* **2013**, *25*, 4035–4042.
59. Sun, H.; You, X.; Deng, J.; Chen, X.; Yang, Z.; Ren, J.; Peng, H. Novel Graphene/Carbon Nanotube Composite Fibers for Efficient Wire-Shaped Miniature Energy Devices. *Adv. Mater.* **2014**, *26*, 2868–2873.
60. Zhang, D.; Miao, M.; Niu, H.; Wei, Z. Core-Spun Carbon Nanotube Yarn Supercapacitors for Wearable Electronic Textiles. *ACS Nano* **2014**, *8*, 4571–4579.